Effect of Alemtuzumab on Intestinal Intraepithelial Lymphocytes and Intestinal Barrier Function in Cynomolgus Model

Lin-Lin Qu[1], Ya-Qing Lyu[1], Hai-Tao Jiang[1], Ting Shan[2], Jing-Bin Zhang[2], Qiu-Rong Li[2], Jie-Shou Li[2]

[1]Department of Biliary Surgery, The Affiliated Hospital of Qingdao University, Qingdao, Shandong 266000, China
[2]Department of General Surgery, Institute of General Surgery, Jinling Hospital, Nanjing, Jiangsu 210002, China

Abstract

Background: Alemtuzumab has been used in organ transplantation and a variety of hematologic malignancies (especially for the treatment of B-cell chronic lymphocytic leukemia). However, serious infectious complications frequently occur after treatment. The reason for increased infections postalemtuzumab treatment is unknown at this stage. We explore the effect of alemtuzumab on intestinal intraepithelial lymphocytes (IELs) and intestinal barrier function in cynomolgus model to explain the reason of infection following alemtuzumab treatment.
Methods: Twelve male cynomolguses were randomly assigned to either a treatment or control group. The treatment group received alemtuzumab (3 mg/kg, intravenous injection) while the control group received the same volume of physiological saline. Intestinal IELs were isolated from the control group and the treatment group (on day 9, 35, and 70 after treatment) for counting and flow cytometric analysis. Moreover, intestinal permeability was monitored by enzymatic spectrophotometric technique and enzyme-linked immunosorbent assay.
Results: The numbers of IELs were decreased significantly on day 9 after treatment compared with the control group ($0.35 \pm 0.07 \times 10^8$ and $1.35 \pm 0.09 \times 10^8$, respectively; $P < 0.05$) and were not fully restored until day 70 after treatment. There were significant differences among four groups considering IELs subtypes. In addition, the proportion of apoptotic IELs after alemtuzumab treatment was significantly higher than in the control group (22.01 ± 3.67 and 6.01 ± 1.42, respectively; $P < 0.05$). Moreover, the concentration of D-lactate and endotoxin was also increased significantly on day 9 after treatment.
Conclusions: Alemtuzumab treatment depletes lymphocytes in the peripheral blood and intestine of cynomolgus model. The induction of apoptosis is an important mechanism of lymphocyte depletion after alemtuzumab treatment. Notably, intestinal barrier function may be disrupted after alemtuzumab treatment.

Key words: Alemtuzumab; Barrier Function; Infection; Intestinal Intraepithelial Lymphocytes; Lymphocyte Depletion

Introduction

Targeted monoclonal antibody (mAb) therapy has become a standard treatment in a number of hematologic malignancies and organ transplantation.[1,2] Alemtuzumab is a humanized mAb targeting the cell surface antigen CD52, which is expressed on more than 95% of all normal B lymphocytes, T lymphocytes, and monocytes.[3] Owing to its triggering of antibody-dependent cell-mediated cytotoxicity, the activation of the complement cascade (complement-dependent cytotoxicity) and induction of apoptosis, alemtuzumab has been used in organ transplantation and a variety of hematologic malignancies (especially for the treatment of B-cell chronic lymphocytic leukemia [B-CLL]).[4,5] Despite many improvements in short-term results following alemtuzumab treatment over the past decade, infection and mobility after treatment are far from ideal.[6] It was reported that more varied, serious infectious complications occurred in patients receiving alemtuzumab.[7,8] However, the reason for infection following alemtuzumab treatment remains unknown.

Intestinal intraepithelial lymphocytes (IELs) maintain intestinal mucosa homeostasis and serve as an immunological barrier against a wide range of infectious agents in the gut lumen.[9] However, it is not clear whether IELs are affected while patients are receiving alemtuzumab. Our previous studies have indicated that anti-mouse CD52 mAbs could induce IELs to apoptosis and result in depletion of IELs.[10] However, there are differences in CD52 peptide sequences between mice and humans.[11] Notably, it was reported that human epitopes were well-conserved in apes, mostly conserved in old world monkeys, but only sometimes conserved in new world monkeys.[12] Therefore, the cynomolgus is the ideal animal model for the alemtuzumab studies.

Access this article online

Quick Response Code:

Website: www.cmj.org

DOI: 10.4103/0366-6999.151675

Address for correspondence: Prof. Jie-Shou Li, Department of General Surgery, Institute of General Surgery, Jinling Hospital, Nanjing, Jiangsu 210002, China
E-Mail: lijieshounju@126.com

In this study, we originally report the effect of alemtuzumab on cynomolgus' IELs and intestinal barrier function with the aim of helping to eliminate infection complicatious postalemtuzumab treatment.

Methods

Animals and experimental design

Juvenile outbred male cynomolgus monkeys, seronegative for simian immunodeficiency virus and herpes B virus, were obtained from the Academy of Military Medical Sciences (AMMS, Beijing, China) and kept in the individual primate facility. These monkeys were aged between 3 and 5 years old with a weight of 3–7 kg. The monkeys were given water *ad libitum*. Biscuits were given twice daily and supplemented with fruit, vegetables, and compound high-nutrition monkey food. The animals received humane care according to the principles set forth in the 'Guide for the Care and Use of Laboratory Animals' from AMMS, the Principles of laboratory animal care (NIH publication No. 86-23, revised 1985) and the American Society of Primatologists Principles for the Ethical Treatment of Nonhuman Primates. No animals were sacrificed in this study.

According to the alemtuzumab product data sheet, a marked reduction in lymphocyte count should occur when animals receive doses of 1 mg/kg mAb or higher. Moreover, it was reported that at a 3 mg/kg dose, there were no major effects on the cardiovascular or respiratory systems. Therefore, all cynomolgus were administered alemtuzumab (MabCampath, Bayer-Schering, Berlin, Germany), at a dose of 3 mg/kg by intravenous injection.

Body weights were determined prior to alemtuzumab administration and after treatment every day for the duration of the study. To mimic the clinical setting and better observe the monkeys for adverse drug effects, blood sampling was conducted on nonanesthetized animals. Before the operation, the cynomolgus were transferred to a sterile operating room. The surgical area was shaved and prepped in an aseptic fashion, usually with iodine solution. The blood pressure, heart rate, respiration, and temperature of cynomolgus were directly monitored with a multi-parameter monitor in real time. After being anesthetized with ketamine (5 mg/kg) and xylidinothiazoline (1 mg/kg), sections of small intestine and colon were obtained by enterectomy from the control group and treatment group on day 9, 35, and 70 after treatment. All surgical incisions were sutured closed, bandaged, and dressings changed on alternate days until the wounds healed.

Animal screening test and immunotherapy

A single autosomal dominant gene is responsible for heterogeneous expression. It means that erythrocytes in cynomolgus are either all CD52 positive or all CD52 negative. Therefore, to avoid hemolysis after mAb treatment, only the cynomolgus whose erythrocytes did not express the CD52 antigen were selected for the trial.

Briefly, 2 ml peripheral blood was obtained by venipuncture from the saphenous vein of 30 healthy cynomolgus and overlaid on 2 ml Ficoll-Hypaque. The gradients were centrifuged at 400 ×*g* for 20 min. After discarding the supernatant, the cell pellets were diluted with Ca^{2+}, Mg^{2+}-free phosphate buffered saline (PBS) to adjust the concentration to 1×10^6 erythrocytes/ml. Purified single-cell erythrocyte suspensions were labeled according to a single color staining procedure using fluorescein isothiocyanate (FITC)-labeled CD 52 mAbs (CF1D12, Invitrogen, Life Technologies, Carlsbad, CA, USA). Appropriate isotype-matched mAbs were used as negative controls. Labeled cells with the forward and side light scatter properties of erythrocytes were analyzed on an FACScan flow cytometer (Becton Dickinson, Franklin Lakes, NJ, USA).

Peripheral blood lymphocyte counts

Blood samples were taken by venipuncture from the saphenous vein of the enrolled cynomolgus. Total blood lymphocyte counts were analyzed using a Cell-Dyne 1300 automated blood counter (Abbott Laboratories, Chicago, IL, USA). The cell counts were defined as the number of leukocytes of volume 40–100 fl detected by the counter in the respective specimens; counts are expressed as cells/L.

Isolation of intestinal intraepithelial lymphocytes

Intraepithelial lymphocytes were isolated according to a modification of previously published methods.[13] Ten centimeters of ileums were obtained from cynomolgus after anesthesia. The fecal material was flushed with cold Roswell Park Memorial Institute (RPMI)-1640 medium containing 5% fetal calf serum (FCS; Sijiqing, Hangzhou, China). The external vasculature and Peyer's patches were removed from the intestinal segments. The intestines were opened longitudinally, cut into 5-mm^2 fragments and transferred to 50-ml plastic conical centrifuge tube. After tissue pieces had settled, the medium was removed by suctioning and replaced with 20 ml PBS, followed by 30 ml Hanks' balanced salt solution (HBSS) containing 0.75 mmol/L ethylenediamine tetra acetic acid (EDTA), 100 U/ml penicillin 100 mg/ml gentamicin, 25 mmol/L HEPES buffer, and 5% FCS. The tissue suspension was transferred to a 150-ml flask and shaken rapidly 300 r/min for 30 min. The cell suspension was washed twice in complete RPMI with 5% FCS and stored on ice. Fresh HBSS–EDTA was added, and the process repeated. The harvested tissue slurries were pooled and passed through 80- and 400-screen mesh trap valve in turn to prepare a single-cell suspension. The cell suspensions were transferred into a 50-ml tube and centrifuged for 10 min at 400 × *g*. After remove the supernatant, cell pellets were esuspended in 2 ml of 35% (v/v) isotonic Percoll and layered onto 2 ml of 60% isotonic Percoll in 15-ml centrifuge tubes. The gradients were centrifuged at 800 × *g* for 20 min. The intercellular layer between 60% Percoll and 35% Percoll was drawn-off and washed twice with RPMI-1640 medium containing 5% FCS. The cell pellet was resuspended in RPMI-1640 medium containing 5% FCS and counted using a hemocytometer.

Flow cytometric analysis

Cells from the above preparations were diluted to 0.5–1 × 10^6 cells/ml and labeled according to the single-, two-, or three-color staining procedure using FITC, allophycocyanin (APC), Perp-cy5.5, and phycoerythrin (PE)-labeled mAbs, including CD45-Perp-cy5.5, CD3-APC (BD Pharmingen, San Diego, CA, USA), CD8-PE, CD4-FITC, T-cell receptor (TCR) αβ-PE, TCR γδ-PE, CD20-PE (e-Bioscience, San Diego, CA, USA). Appropriate isotype-matched mAbs were used as negative controls. Labeled IELs were analyzed on an FACScan flow cytometer (Becton Dickinson, CA, USA).

Cell apoptosis

Apoptosis of IELs was determined using the apoptosis assay kit No. 2 (Molecular Probes, Life Technologies, Carlsbad, CA, USA) in accordance with the manufacturer's instructions. Briefly, the isolated IELs were washed in cold PBS, and the negative control was diluted in ×1 annexin-binding buffer. The IELs of the assay group were centrifuged, the supernatant discarded, and the pellet resuspended in ×1 annexin-binding buffer. The cell density was adjusted to 0.5–1 × 10^6 cells/ml. 5 μl Alexa Fluor 488 annexin V and 1 μl propidium iodide (PI) working solution were added to the cell suspension. After incubation at room temperature for 15 min, 400 μl of ×1 annexin-binding buffer was added to the cell suspension, mixed gently, and the labeled cells analyzed on an FACScan flow cytometer.

Gross morphology and histology of the intestine

Tissue specimens from the ileum adjoining the ileocecal junction were taken and opened longitudinally. After the fecal material had been flushed with RPMI-1640 medium containing 5% FCS, gross morphology was taken by a digital camera. The tissue segments for histology were fixed in 10% formaldehyde solution, embedded in paraffin, sectioned at 5 μm and stained with hematoxylin and eosin (H and E).

Serum D-lactate detection

The concentration of D-lactate in cynomolgus serum was determined following the protocol of the detection kit (GMS70095.3 v.A, Genmed Scientific Inc., Shanghai, China). Briefly, the serum was added to 100 μl treating solution and centrifuged at 700 × *g* for 15 min. Then 20 μl supernatant was collected and 780 μl reagent B, 100 μl reagent C, 100 μl reagent D added sequentially. After incubation at room temperature for 5 min, the D-lactate concentration was determined by an enzymatic spectrophotometric technique. Determination of the background was made in the same way. D-lactate concentration was calculated using a standard curve.

Measurement of endotoxin in plasma

The blood samples were centrifuged for 15 min at 10,000 × *g*. The supernatant was assayed for endotoxin levels by enzyme-linked immunosorbent assay kits (R and D Systems, Minneapolis, MN, USA) according to the instructions. The absorbance at 450 nm was determined with a microplate reader (Tecan's, Sunrise, Unterberg Strasse IA, Austria).

Transmission electron microscopy

The colon specimens were fixed in 2% glutaraldehyde and fixed in 1% osmium tetroxide. After dehydrated with stepwise ethanol and embedded in Epon 812, ultrathin sections were cut and stained with uranyl acetate and lead citrate. The ultrastructures were examined using a Hitachi JEM 1200-EX transmission electron microscope (TEM) (Hitachi, Tokyo, Japan) at an accelerating voltage of 100 kV and a magnification of 20,000.

Statistical analysis

Results are expressed as the mean ± standard deviation (SD). Analysis of variance (ANOVA) and Dunnet *t*-test were used to determine the significance of differences between groups. Data were analyzed using SPSS 13.0 software (SPSS Inc, IL, USA). A $P < 0.05$ was considered statistically significant.

Results

Animal screening

To avoid hemolysis after alemtuzumab treatment; we used flow cytometry to screen for cynomolgus whose erythrocytes did not express CD52 antigen. Twelve cynomolguses were enrolled in our study of the 30 screened cynomolguses and randomly assigned to either a treatment or control group in accordance with the random number table.

Lymphocyte depletion in blood and intestine

To investigate the depletion of lymphocytes in the blood, an automated blood counter was used to count the lymphocytes. As shown in Figure 1, the number of lymphocytes decreased

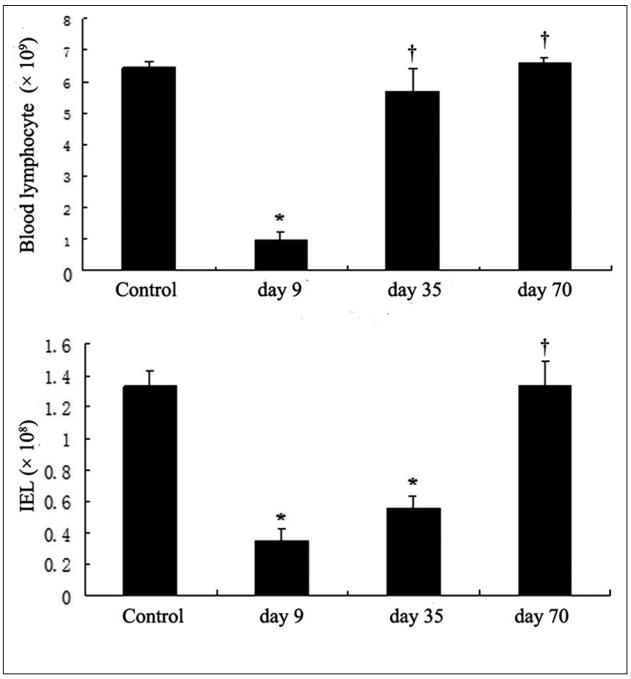

Figure 1: Depletion of lymphocytes in the peripheral blood and colon of cynomolgus monkeys by alemtuzumab treatment. The number of lymphocytes in blood and intestine epithelium was examined on day 9, 35 and 70 after treatment and in the control group. *$P < 0.05$ compared with control group; †$P > 0.05$ compared with control group.

immediately and sharply after alemtuzumab treatment, and was reduced to a minimum by day 9 after treatment. Furthermore, the lymphocyte numbers were not restored until day 35 after treatment. There was no significance of lymphocyte count between the day 35 group and the control group, indicating that the number of lymphocytes in the blood were restored entirely by day 35.

In addition, to determine whether alemtuzumab had an effect on IELs, we isolated and quantified the number of IELs with a hemocytometer [Figure 1]. It was also noted that IELs had sharply dropped to the lowest level on day 9 following alemtuzumab treatment, with a significant difference between treatment and control groups ($0.35 \pm 0.07 \times 10^8$ and $1.35 \pm 0.09 \times 10^8$, respectively; $P < 0.05$). The IELs of the treatment group were restored entirely by day 70. These findings confirmed the depletion of IELs after alemtuzumab treatment.

Intraepithelial lymphocytes subtypes

Following the isolation technique of Zeitz *et al.*,[13] we obtained IELs with high levels of purity and viability (>90%). We used flow cytometry to investigate the phenotype of the IELs isolated. The results showed that the percentage of TCR $\gamma\delta^+$ and $CD20^+$ cells decreased after alemtuzumab treatment while TCR $\alpha\beta^+$ and $CD8^+$ T-cell increased significantly after treatment ($P < 0.05$, Table 1).

Intraepithelial lymphocytes apoptosis

Induction of apoptosis is one of the most important mechanisms of lymphocyte depletion after treatment with alemtuzumab. Therefore, we examined the effect of alemtuzumab on the proportion of apoptotic IELs. As seen in Figure 2, a significant increase in the proportion of apoptotic IELs was observed on day 9 after treatment compared with the control group (22.01 ± 3.67 and 6.01 ± 1.42, respectively; $P < 0.05$). There was no significant difference in the proportion of apoptotic IELs between day 70 after treatment and the control group.

Gross morphology and histology

In the present study, the difference in thickness of the intestinal wall and number of mucosal folds was shown in the ileum of cynomolgus after alemtuzumab treatment [Figure 3a]. The intestine of cynomolgus in the control group had more abundant folds and thicker intestinal wall. However, after being treated for 9 days, the ileums of cynomolgus appeared to have a thinner intestinal wall and the mucosal folds nearly disappeared. On day 35, after alemtuzumab treatment, sporadic mucosal fold emerged, however, the intestinal wall still appeared very thin. As shown in Figure 4a, the ileum showed normal mucosal folds by 70 days after treatment.

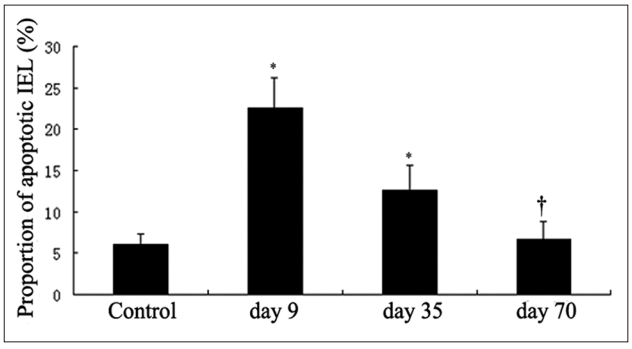

Figure 2: Proportion of apoptotic intraepithelial lymphocytes (IELs). The result is representative of those obtained with 3 cynomolguses per group. The proportion of apoptotic IELs after alemtuzumab treatment for 9 days was significantly higher than the control group. *$P < 0.05$ compared with control group; †$P > 0.05$ compared with control group.

We next investigated the effect of alemtuzumab on the intestine by examining H and E-stained sections from the control and treatment groups [Figure 3b]. H and E staining of the ileum and colon of the control group revealed intact villi and regular compactly arrayed epithelium. In contrast, the ileum and colon villi atrophied after treatment. Moreover, the epithelium demonstrated an irregular arrangement and formed branch-like prominences. Notably, on day 70 after treatment, restored villi were observed in the ileum and colon.

Intestinal permeability

To investigate whether the intestinal barrier may be destroyed, we measured D-lactate in cynomolgus serum as an index of small intestinal permeability [Figure 4a]. Compared with the control group, alemtuzumab-treated cynomolgus showed a significant increase in intestinal permeability on day 9 after treatment as measured by serum D-lactate concentration (0.243 ± 0.080 and 0.847 ± 0.081 mmol/L, respectively; $P < 0.05$). However, the concentration of D-lactate decreased to the level of the control group by day 70 after treatment. No significant differences in of D-lactate concentration were observed between the day 70 posttreatment group and the control group (0.167 ± 0.012 and 0.243 ± 0.080 mmol/L, respectively; $P > 0.05$).

Level of endotoxin in plasma

As shown in Figure 4b, the levels of endotoxin increased significantly on day 9 after treatment Compared with the control group (1.255 ± 0.035 and 0.238 ± 0.024 EU/ml, respectively, $P < 0.05$). The levels of endotoxin decreased gradually to the normal level until day 70 after treatment (0.241 ± 0.036 and 0.238 ± 0.024 EU/ml, respectively, $P > 0.05$).

Alteration of tight junction ultrastructure

Tight junctions (TJs) play an important regulatory role in barrier function. To assess the effects of alemtuzumab on TJ ultrastructure, TEM was performed on the colon. It was showed in Figure 5, that TEM of the colon revealed an intact TJ structure in cynomolgus of the control group. The ultrastructure of TJs was altered in animals after intravenously guttae with alemtuzumab for 9 and 35 days. The desmosome disappeared, and TJ membrane fusions were lost. It indicated that the normal TJ morphology was disrupted after treatment. On the 70th day after treatment, the desmosome and TJ membrane fusions reemerged, which indicated that TJ has recovered [Figure 5].

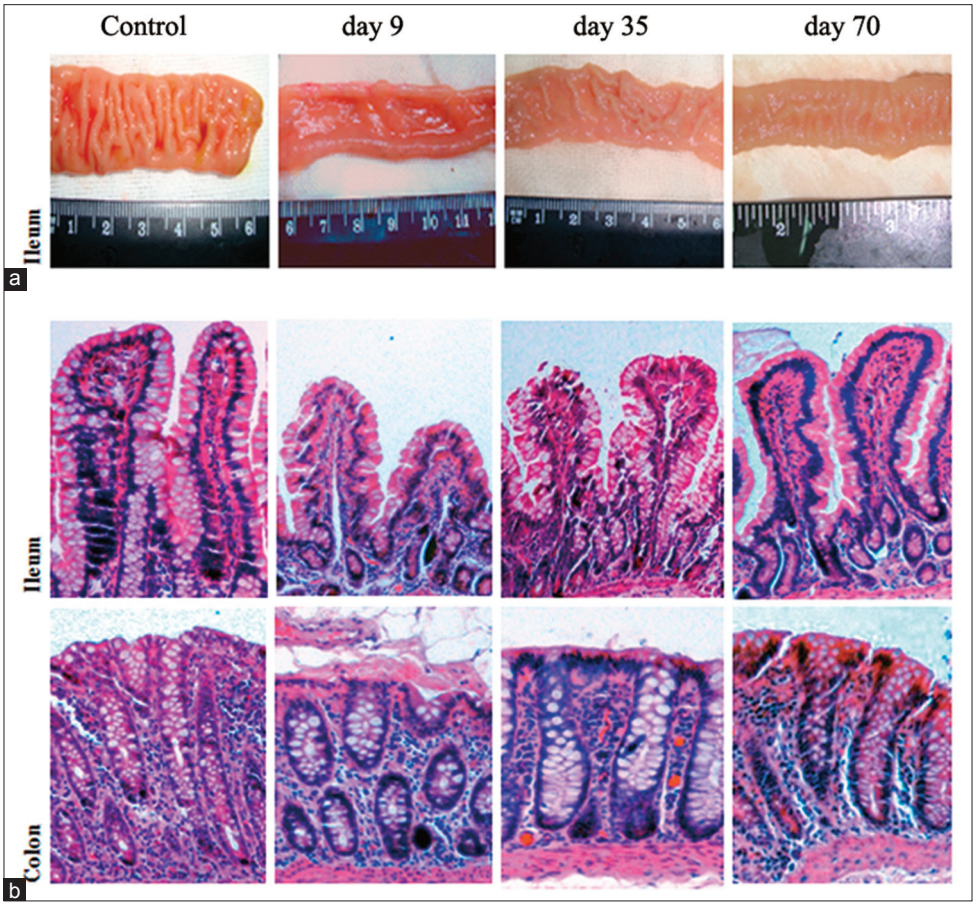

Figure 3: Gross morphology (a) and histology (b) of cynomolgus treated with physical saline or alemtuzumab. Representative H and E-stained histological sections. The results are representative of those obtained with 3 cynomolguses of each group. Original magnification, ×40.

Table 1: Phenotypes of IELs in the control group and the treatment group (%)

Cell population	Control group	Treatment group		
		Day 9	Day 35	Day 70
$CD8^+CD4^-$	68.83 ± 1.76	70.03 ± 2.35	83.9 ± 0.81*	67.94 ± 1.88
$CD8^-CD4^+$	28.59 ± 1.52	27.54 ± 6.44	27.91 ± 3.13	28.33 ± 3.19
TCR $\alpha\beta^+$	23.37 ± 4.59	54.15 ± 5.19*	35.96 ± 2.24*	23.82 ± 2.09
TCR $\gamma\delta^+$	11.05 ± 1.66	5.61 ± 0.35*	7.54 ± 0.86*	10.56 ± 0.54
$CD20^{+\dagger}$	6.59 ± 1.12	1.58 ± 0.40*	2.23 ± 1.18*	6.53 ± 1.22

Data are presented as the percentage of cells with respect to the total number of $CD3^+$ cells; $n = 3$ per group. *$P < 0.05$ versus the control group; †The value is the percentage of $CD3^-CD20^+$ cells. TCR: T-cell receptor; IELs: Intestinal intraepithelial lymphocytes.

Discussion

Alemtuzumab is a recombinant DNA-derived humanized mAb, which is used therapeutically in B-CLL and organ transplantation, including kidney, liver, and intestine transplantation.[14-17] Although excellent short-term graft survival with a decrease in the incidence of acute rejection has been reported, alemtuzumab anti-rejection therapy is far from optimal.[18,19] Transplant-related mortality after alemtuzumab treatment is mainly caused by rejection and infection.[20] Serious, sometimes fatal, bacterial, viral, fungal, and protozoan infections have been reported in patients receiving alemtuzumab therapy. Unfortunately, the mechanism of infection complications remains unclear. Our study originally investigated the effect of alemtuzumab on IELs and intestinal barrier function in a cynomolgus model in order to elucidate the mechanism of infectious complications after alemtuzumab treatment.

Intraepithelial lymphocytes constitute a unique population of lymphoid cells residing as single cells between intestinal epithelial cells.[21] They are active as the first line of specific defense to encounter invading infectious agents that have entered the body via the local epithelial surface. IELs play an important role in the maintenance of mucosal homeostasis and the integrity of epithelial tissues.[22] The IELs are mainly comprised of T-cell and can be divided into two groups according to the TCR phenotype, namely TCR $\alpha\beta^+$ and TCR $\gamma\delta^+$ cells. In this study, we examined the effect of alemtuzumab on the number and phenotype of IELs *in vivo*. Compared with the limited depletion of anti-CD52 mAb on IELs in a mouse model,[10] more powerful clearance of IELs caused by alemtuzumab was observed in this study. It was found that IELs decreased significantly after treatment, accompanied by the decline of lymphocytes in the blood. Induction of apoptosis, antibody-dependent cell cytotoxicity, and complement-mediated cell death (CDC) is the proposed mechanism of action of alemtuzumab.[4] In our study, we found

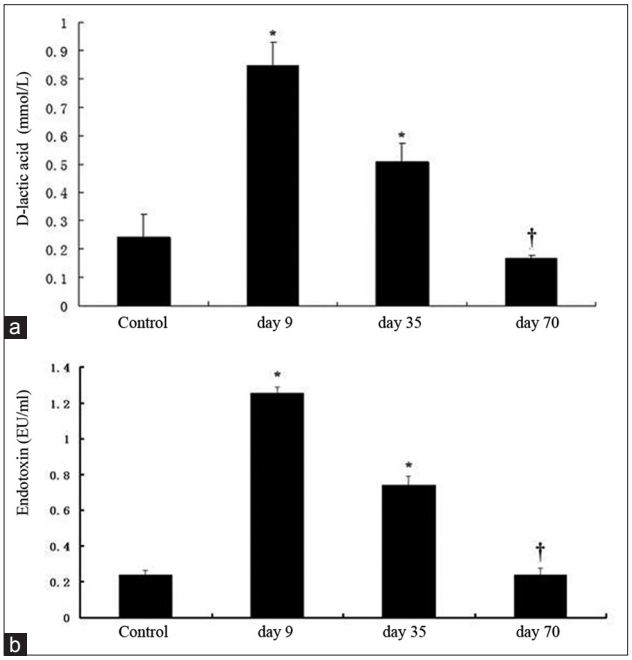

Figure 4: The level of D-lactate and endotoxin in cynomolgus serum. The level of D-lactate could reflect the intestinal permeability. *$P < 0.05$ compared with the control group; †$P > 0.05$ compared with control group.

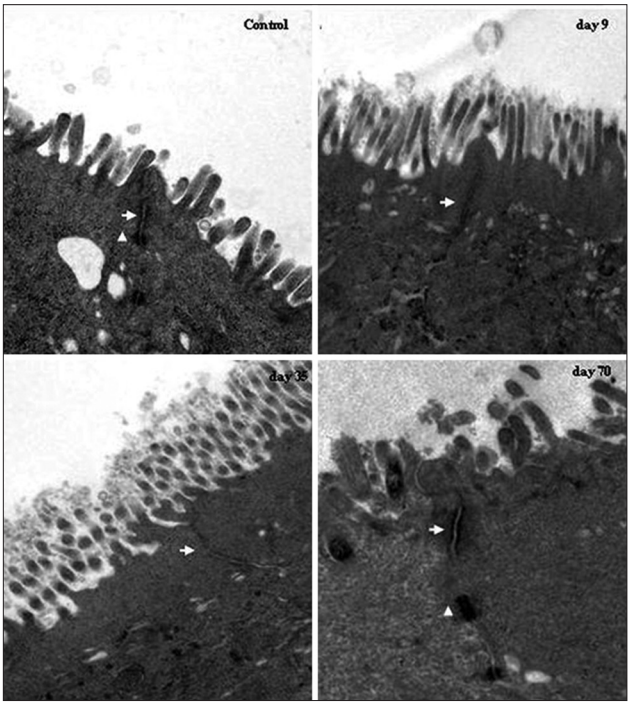

Figure 5: Modulation of tight junctions (TJs) structure after alemtuzumab treatment. In controls, TJ and desmosome displayed an intact structure. On the 9th and the 35th day after treatment, alteration of TJ ultrastructure was observed, and desmosome disappeared. The TJ structure recovered on the 70th day after treatment. Arrows: TJs; arrowheads: Desmosomes (Original magnification × 20000).

that the percentage of apoptotic IELs increased significantly after alemtuzumab treatment. Therefore, it can be inferred that induction of apoptosis played an important role in the mechanism of IELs depletion caused by alemtuzumab. We subsequently examined the phenotypes of IELs after alemtuzumab treatment. The percentage of $CD4^+$ and $CD8^+$ IELs were not changed on day 9 after treatment while the percentage of $CD8^+$ IELs increased significantly on day 35 after treatment. A possible explanation may be that alemtuzumab induces equal depletion of the $CD4^+$ and $CD8^+$ IELs by the populations recovered differently. The decrease of $CD20^+$ IELs signifies that the alemtuzumab could also induce the depletion of B-cell. Moreover, it was also noted that TCR $\gamma\delta^+$ IELs decreased significantly after alemtuzumab treatment. Recent studies have shown that TCR $\gamma\delta^+$ IELs could regulate the generation and differentiation of EC. Abnormal EC turnover and function was found in mice lacking TCR γδ IELs.[23] Therefore, we put forward the hypothesis that the intestinal barrier function is disrupted after alemtuzumab treatment because of the depletion of IELs.

It was reported that diarrhea and infection are potential complications after alemtuzumab therapy.[24] When patients suffering from lymphoma were treated with alemtuzumab, abnormal, disarrayed epithelium was found after histological examination of the colon, with bacilli attaching to the surfaces of damaged epithelial cells.[25] Our study showed that in addition to the depletion of IELs, intestinal walls became fairly notably, and atrophica ileum and colon epithelium were observed on day 9 after treatment. Moreover, the brush border of colon villi became discontinuous. This suggests that the treatment with alemtuzumab may cause a profound depletion of intestinal IELs that predisposes the intestinal mucosa to disruption.

D-lactate is a specific by-product of bacterial metabolism; it is neither produced nor metabolized by mammalian cells. When the mucosal barrier of the gut begins to break down, D-lactate crosses the mucosal barrier in large quantities, and the concentration of D-lactate becomes elevated in peripheral blood serum.[26] In our study, we found that the D-lactate concentrations and levels of endotoxin were increased significantly on day 9 after alemtuzumab treatment and gradually decreased to the normal level by day 70.

Our present findings originally demonstrated that the changes of TJ ultrastructure and protein expression. After alemtuzumab treatment, the ultrastructure of TJ was not intact, and the electron-dense materials diminished. Until 70 days after treatment, the morphology of TJ recovered and the electron–dense material reoccurred. It means that the intestine barrier function was destroyed following alemtuzumab treatment.

In conclusion, our study demonstrated that the alemtuzumab induces IELs apoptosis and leads to IELs depletion. The different subtypes of IELs were also all affected after treatment. The reduction of IELs may result in disruption of the intestine barrier, which could explain why bacterial complications frequently occur after alemtuzumab therapy. Therefore, to improve patient outcomes, more attention should be paid by clinicians to protection of intestinal barrier function. However, the precise mechanism by which alemtuzumab disrupts the intestinal barrier requires further investigation.

References

1. Demko S, Summers J, Keegan P, Pazdur R. FDA drug approval summary: Alemtuzumab as single-agent treatment for B-cell chronic lymphocytic leukemia. Oncologist 2008;13:167-74.
2. Ho VT, Cutler C. Current and novel therapies in acute GVHD. Best Pract Res Clin Haematol 2008;21:223-37.
3. Rowan W, Tite J, Topley P, Brett SJ. Cross-linking of the CAMPATH-1 antigen (CD52) mediates growth inhibition in human B- and T-lymphoma cell lines, and subsequent emergence of CD52-deficient cells. Immunology 1998;95:427-36.
4. Villamor N, Montserrat E, Colomer D. Mechanism of action and resistance to monoclonal antibody therapy. Semin Oncol 2003;30:424-33.
5. Fraser G, Smith CA, Imrie K, Meyer R, Hematology Disease Site Group of Cancer Care Ontario's Program in Evidence-based Care. Alemtuzumab in chronic lymphocytic leukemia. Curr Oncol 2007;14:96-109.
6. Novitzky N, Rouskova A. Infectious complications following T-cell depleted hematopoietic stem-cell transplantation. Cytotherapy 2001;3:165-73.
7. Martin SI, Marty FM, Fiumara K, Treon SP, Gribben JG, Baden LR. Infectious complications associated with alemtuzumab use for lymphoproliferative disorders. Clin Infect Dis 2006;43:16-24.
8. Zanfi C, Lauro A, Cescon M, Dazzi A, Ercolani G, Grazi GL, *et al.* Daclizumab and alemtuzumab as induction agents in adult intestinal and multivisceral transplantation: Rejection and infection rates in 40 recipients during the early postoperative period. Transplant Proc 2010;42:35-8.
9. Lepage AC, Buzoni-Gatel D, Bout DT, Kasper LH. Gut-derived intraepithelial lymphocytes induce long term immunity against *Toxoplasma gondii*. J Immunol 1998;161:4902-8.
10. Qu L, Li Q, Jiang H, Gu L, Zhang Q, Wang C, *et al.* Effect of anti-mouse CD52 monoclonal antibody on mouse intestinal intraepithelial lymphocytes. Transplantation 2009;88:766-72.
11. Hale G. CD52 (CAMPATH1). J Biol Regul Homeost Agents 2001;15:386-91.
12. Loisel S, Ohresser M, Pallardy M, Daydé D, Berthou C, Cartron G, *et al.* Relevance, advantages and limitations of animal models used in the development of monoclonal antibodies for cancer treatment. Crit Rev Oncol Hematol 2007;62:34-42.
13. Zeitz M, Greene WC, Peffer NJ, James SP. Lymphocytes isolated from the intestinal lamina propria of normal nonhuman primates have increased expression of genes associated with T-cell activation. Gastroenterology 1988;94:647-55.
14. Tzakis AG, Kato T, Nishida S, Levi DM, Madariaga JR, Nery JR, *et al.* Preliminary experience with campath 1H (C1H) in intestinal and liver transplantation. Transplantation 2003;75:1227-31.
15. Stanglmaier M, Reis S, Hallek M. Rituximab and alemtuzumab induce a nonclassic, caspase-independent apoptotic pathway in B-lymphoid cell lines and in chronic lymphocytic leukemia cells. Ann Hematol 2004;83:634-45.
16. Nainani N, Singh N, Shanahan T, Damodar A, Parimoo N, Ummadi S, *et al.* Cross reactive epitope group antibodies in sensitized kidneys transplant recipients was associated with early acute antibody mediated rejection. Transpl Immunol 2009;20:113-7.
17. Lü TM, Yang SL, Wu WZ, Tan JM. Alemtuzumab induction therapy in highly sensitized kidney transplant recipients. Chin Med J 2011;124:664-8.
18. Nückel H, Frey UH, Röth A, Dührsen U, Siffert W. Alemtuzumab induces enhanced apoptosis *in vitro* in B-cells from patients with chronic lymphocytic leukemia by antibody-dependent cellular cytotoxicity. Eur J Pharmacol 2005;514:217-24.
19. Shapiro R, Basu A, Tan H, Gray E, Kahn A, Randhawa P, *et al.* Kidney transplantation under minimal immunosuppression after pretransplant lymphoid depletion with Thymoglobulin or Campath. J Am Coll Surg 2005;200:505-15.
20. Arnold R, Bunjes D, Wiesneth M, Hertenstein B, Theobald M, Heimpel H, *et al. In vitro* and *in vivo* depletion of T cells. Bone Marrow Transplant 1993;12 Suppl 3:S11-2.
21. Beagley KW, Husband AJ. Intraepithelial lymphocytes: Origins, distribution, and function. Crit Rev Immunol 1998;18:237-54.
22. Cheroutre H, Kronenberg M. Mucosal T lymphocytes – Peacekeepers and warriors. Springer Semin Immunopathol 2005;27:147-65.
23. Komano H, Fujiura Y, Kawaguchi M, Matsumoto S, Hashimoto Y, Obana S, *et al.* Homeostatic regulation of intestinal epithelia by intraepithelial gamma delta T cells. Proc Natl Acad Sci U S A 1995;92:6147-51.
24. Tang SC, Hewitt K, Reis MD, Berinstein NL. Immunosuppressive toxicity of CAMPATH1H monoclonal antibody in the treatment of patients with recurrent low grade lymphoma. Leuk Lymphoma 1996;24:93-101.
25. Goteri G, Rupoli S, Tassetti A, Pulini S, Morichetti D, Filosa A, *et al.* Severe diarrhoea during Campath-1H treatment for refractory cutaneous T-cell lymphoma. Ann Hematol 2006;85:617-9.
26. Murray MJ, Barbose JJ, Cobb CF. Serum D(-)-lactate levels as a predictor of acute intestinal ischemia in a rat model. J Surg Res 1993;54:507-9.

Received: 19-07-2014 **Edited by:** Yuan-Yuan Ji

How to cite this article: Qu LL, Lyu YQ, Jiang HT, Shan T, Zhang JB, Li QR, Li JS. Effect of Alemtuzumab on Intestinal Intraepithelial Lymphocytes and Intestinal Barrier Function in Cynomolgus Model. Chin Med J 2015;128:680-6.

Source of Support: This work was supported by grants from the National Basic Research Program (973 Program) in China (No. 2007CB513005 and 2009CB522405), Shangdong Province Young and Middle-Aged Scientists Research Awards Fund (No. BS2011YY004), the Key Project of National Natural Science Foundation in China (No. 30830098), National Key Project of Scientific and Technical Supporting Programs Funded by Ministry of Science and Technology of China (No. 2008BAI60B06), the National Natural Science Foundation in China (No. 30672061), the Military Scientific Research Fund (No. 0603AM117) and the Gut Barrier Foundation of Jie-Shou Li Academician. **Conflict of Interest:** None declared.